Available online at www.sciencedirect.com
SCIENCE DIRECT®
Carbohydrate Research 338 (2003) 341–352
CARBOHYDRATE RESEARCH
www.elsevier.com/locate/carres

Primary structure of the 2-*O*-methyl-α-L-fucose-containing side chain of the pectic polysaccharide, rhamnogalacturonan II

John N. Glushka, Mark Terrell, William S. York, Malcolm A. O'Neill, Angela Gucwa, Alan G. Darvill, Peter Albersheim, James H. Prestegard*

Complex Carbohydrate Research Center, Department of Chemistry and Department of Biochemistry and Molecular Biology, The University of Georgia, 220 Riverbend Road, Athens, GA 30602-4712, USA

Received 16 July 2002; accepted 5 November 2002

Abstract

A 2-*O*-methylfucosyl-containing heptasaccharide was released from red wine rhamnogalacturonan II (RG-II) by acid hydrolysis of the glycosidic linkage of the aceryl acid residue (AceA) and purified to homogeneity by size-exclusion and high-performance anion-exchange chromatographies. The primary structure of the heptasaccharide was determined by glycosyl-residue and glycosyl-linkage composition analyses, ESIMS, and by ^{1}H and ^{13}C NMR spectroscopy. The NMR data indicated that the pyranose ring of the 2,3-linked L-arabinosyl residue is conformationally flexible. The L-Ara*p* residue was confirmed to be α-linked by NMR analysis of a tetraglycosyl-glycerol fragment, [α-L-Ara*p*-(1→4)-β-D-Gal*p*-(1→2)-α-L-Ace*f*A-(1→3)-β-L-Rha*p*-(1→3)-Gro], generated by Smith degradation of RG-II. Our data together with the results of a previous study,[1] establish that the 2-*O*-Me Fuc-containing nonasaccharide side chain of wine RG-II has the structure (Api ≡ apiose):

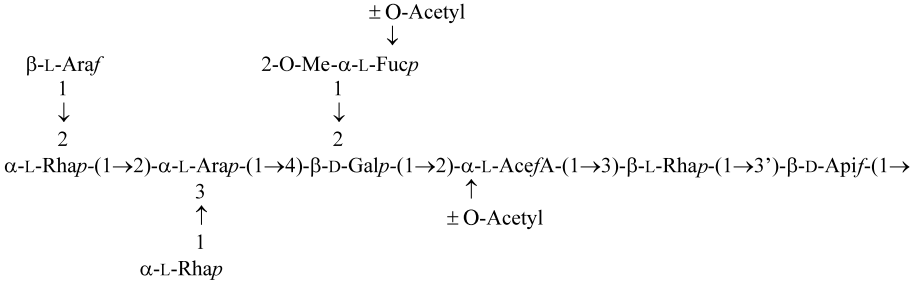

Data are presented to show that in Arabidopsis RG-II the predominant 2-*O*-MeFuc-containing side chain is a mono-*O*-acetylated heptasaccharide that lacks the non-reducing terminal β-L-Ara*f* and the α-L-Rha*p* residue attached to the O-3 of Ara*p*, both of which are present on the wine nonasaccharide.

Keywords: Cell wall; Oligosaccharide; NMR; Mass spectrometry; Arabinose flexibility

1. Introduction

Rhamnogalacturonan II (RG-II) is a low-molecular weight (5–10 kDa), structurally well-defined, complex pectic polysaccharide that is released from plant cell walls by treatment with endo-α-(1→4)-polygalacturonase.[2,3] RG-II is also present in the commercial enzyme preparation Pectinol AC[4] and in red wine.[5,6] RG-II exists in the primary cell wall and in wine as a dimer that is cross-linked by a 1:2 borate–diol ester.[6–10] The ester is formed between the apiosyl residue (Api) of the 2-*O*-MeXyl-containing side chain in each RG-II monomer.[11] Dimer formation in vitro is pH dependent and is promoted by divalent cations.[9,11] Somewhat unexpectedly, the stability of the dimer and its in vitro

* Corresponding author. Tel.: +1-706-5426281; fax: +1-706-5424412
E-mail address: jpresteg@ccrc.uga.edu (J.H. Prestegard).

0008-6215/03/$ - see front matter
PII: S0008-6215(02)00461-5

rate of formation are reduced by replacing L-Fuc residues by L-Gal residues.[12] More importantly, these structural changes result in a decrease in borate cross linking of RG-II in muro, which itself is proposed to be responsible for the dwarf phenotype of the Arabidopsis *mur1* mutant.[12] Such results, when taken together with the ability of the dimer to selectively bind heavy metal ions including Pb^{2+}, Sr^{2+}, Ba^{2+}, and La^{3+},[9,12] suggest that the properties of RG-II are determined by its primary structure and solution conformation.

Computer-generated, low-energy structures for the four oligosaccharide side chains of RG-II have been described,[13] although the predicted conformations have not been substantiated with experimental data. The results of an NMR spectroscopic study of monomeric RG-II have been reported,[14] but some of the signal assignments have been questioned.[1] A complete and unambiguous assignment of the ^1H and ^{13}C spectra of RG-II requires that oligosaccharide fragments of this pectic polysaccharide are generated and structurally characterized. Such an approach has been successfully used for the structural characterization of plant cell-wall xyloglucans.[15]

Chemical fragmentation of RG-II has led to the isolation and structural characterization of four structurally different oligoglycosyl side chains,[4,16–21] referred to as side chains A, B, C, and D.[6] Side chain A is a 2-*O*-MeXyl-containing octasaccharide,[21] whereas side chains C and D are the disaccharides β-L-Ara*f*-(1→5)-β-D-Dha-(1→ and α-L-Rha*p*-(1→5)-β-D-Kdo-(1→, respectively.[17,20] Side chain B was reported to be a heptasaccharide containing aceric acid (AceA),[4] although recent evidence suggests that the heptasaccharide may have originated from an octa- or nonasaccharide.[22] Moreover, a high-field NMR spectroscopic analysis of a portion of side chain B generated from wine RG-II has established that the AceA*f* and Gal*p* residues are α and β linked, respectively,[1] and thus the original assignments for the anomeric configurations of these glycosyl residues[4] were incorrect.

We now report the complete assignment of the ^1H and ^{13}C NMR spectra of an aceric acid-containing heptasaccharide and an aceric acid-containing tetraglycosylglycerol fragment generated from wine RG-II by selective acid hydrolysis and by Smith degradation, respectively. These data, together with the results of a previous study,[1] provide a unambiguous primary sequence for side chain B of wine RG-II. Our data indicate that in this oligosaccharide, the 2,3-linked α-L-arabinopyranose residue exhibits multiple conformations, and that the side chain is conformationally dynamic in intact RG-II. We also provide data to show that side chain B exists predominantly as a mono-*O*-acetylated nonasaccharide in wine RG-II and as a mono-*O*-acetylated heptasaccharide in Arabidopsis RG-II, which provides evidence that its structure may vary, depending on the plant source.

2. Experimental

2.1. Generation and isolation of aceric acid-containing side chain B from red wine RG-II

RG-II was isolated from red wine as previously described.[6] A solution of RG-II (5 g) in 2% aq AcOH (500 mL) was incubated for 1.5 h at 100 °C. The solution was cooled and then concentrated to dryness under vacuum. The residue was dissolved in water and freeze-dried, then dissolved in a mixture of H_2O (130 mL) and HOAc (20 mL), followed by the addition of 95% EtOH (850 mL). The resulting mixture was kept at 4 °C for 16 h, and the precipitate that formed was removed by centrifugation. The soluble fraction was concentrated to dryness under vacuum yielding ~200 mg of material. This material was fractionated (~8 mg/run) on a Superdex peptide 10/30/HR column using 50 mM ammonium formate at pH 5 with a 0.6 mL/min flow rate and a HP RI detector. The major peak, which eluted between 23 and 26 min was collected manually and repeatedly freeze dried to remove ammonium formate. The residue was dissolved in H_2O and fractionated (~5 mg/run) by HPAEC using a semiprep CarboPac PA1 column (9 × 250 mm). The column was eluted at 2mL/min with 100 mM NaOH (0–5 min), followed by a gradient (0–200 mM NaOAc, in 100 mM NaOH, 5–30 min). The column was then washed with 800 mM NaOAc in 100 mM NaOH (15 min) and then equilibrated for 15 min with 100 mM NaOH prior to the next injection. The eluant was monitored with a PAD detector, and fractions were collected manually. The major peak (Fraction 4) was desalted using an OnGuard-H^+ ion-exchange cartridge (Dionex) and then freeze-dried. Fraction 4 gave a single peak when chromatographed, using the above gradient at 1 mL/min, on an analytical (4 × 250 mm) CarboPac PA1 column.

2.2. Smith degradation of RG-II

Wine RG-II (150 mg) was de-esterified by treatment for 16 h at 4 °C with 0.1 M NaOH (15 mL). The solution was adjusted to pH 5 with HOAc and then dialyzed (3500 MW cut-off). The de-esterified RG-II (145 mg) was then treated for 45 min at 20 °C with 0.1 M HCl (10 mL) to convert the RG-II to its monomeric form.[9] The solution was dialyzed and freeze-dried. A solution of monomeric RG-II (140 mg) in 50 mM sodium periodate was kept for 48 h at 20 °C in the absence of light.[23] Ethylene glycol (1 mL) was added, and the solution was kept at 20 °C for 1 h to destroy the excess sodium periodate. A solution (10 mL) of $NaBH_4$ (10 mg/mL in 1 M NH_4OH) was then added dropwise, and the mixture was kept for 16 h at room temperature (rt). The excess $NaBH_4$ was destroyed by the addition of

HOAc. The solution was dialyzed and then freeze-dried.

A solution of the periodate-oxidized and $NaBH_4$-reduced RG-II (100 mg) in 0.1 M TFA (25 mL) was kept for 24 h at 40 °C. The solution was concentrated to dryness under a stream of air, and the residual TFA was removed by washing the residue with MeOH (3 × 5 mL). A solution of the residue in 25 mM ammonium formate, pH 6.5 (5 mL) was fractionated on a Q-Sepharose anion-exchange column (2.2 × 10 cm). Neutral material was eluted at 2 mL/min with 25 mM ammonium formate, pH 6.5 (100 mL). The acidic oligoglycoses were eluted with 250 mM ammonium formate, pH 6.5 (200 mL). The acidic fraction was concentrated to dryness under vacuum, dissolved in water (15 mL) and then repeatedly freeze-dried to remove the ammonium formate. A 2-mL solution of the residue in water was filtered (0.2-μm Nylon-66 membrane), and 200-μL portions fractionated by HPAEC on a semipreparative CarboPac 1 column (9 × 250 mm, Dionex Corp, Sunnyvale CA) by eluting at 2 mL/min with 100 mM NaOH (0–5 min), followed by a 0–100 mM NaOAc gradient in 100 mM NaOH (5–45 min), and finally with 800 mM NaOAc in 100 mM NaOH (45–55 min). The eluant was monitored with a pulsed amperometric detector (Dionex Corp) at 30 μamp sensitivity. Fractions were collected manually. The fractions were desalted (5 mL/cartridge) using OnGuard H cartridges (Dionex Corp) and freeze-dried.

2.3. Conversion of the oligoglycoses in Fraction 4 to their corresponding oligoglycosyl alditols

A solution of Fraction 4 (1 mg) in 1 M NH_4OH (100 μL) was treated for 2 h at 20 °C with $NaBD_4$ (250 μL; 10 mg/mL in 1 M NH_4OH) to convert the reducing end of the oligoglycose to a deuterium-labeled alditol. The solution was acidified with HOAc to destroy the excess borodeuteride. The sample was then concentrated to dryness under a flow of nitrogen gas. The residue was treated with MeOH containing 10% HOAc (3 × 250 μL) to remove boric acid, and then with MeOH (3 × 250 μL). A solution of the residue in water (500 μL) was desalted using an OnGuard-H^+ cation exchange cartridge (Dionex Corp) and then freeze-dried. The $NaBD_4$-reduced Fraction 4 was hydrolyzed for 1.5 h at 121 °C with 2 M TFA. The released glycoses were converted to their corresponding alditols by treatment with $NaBH_4$ in 1 M NH_4OH and then per-*O*-acetylated.[24] The acetylated alditols were quantified by GC and analyzed by GC–EIMS to distinguish the H-reduced alditols from the deuterium-labeled alditol that was derived from the reducing glycose of the oligosaccharide.

2.4. Determination of the glycosyl linkage composition of Fraction 4

A solution of Fraction 4 and $NaBH_4$-reduced Fraction (500 μg) in dimethyl sulfoxide (200 μL) were treated for 15 min at 20 °C with NaOH/Me_2SO (200 μL) and CD_3I (100 μL).[25] Deuterated methyl iodide was used so that 2-O-MeFuc could be unambiguously identified by GC–MS. Water (1 mL) was added, and the excess CD_3I was removed by flushing the solution with N_2. Dichloromethane (2 mL) was added, and the organic phase was washed with water (4 × 2 mL). The organic phase containing the methylated oligosaccharides was then concentrated to dryness under a flow of N_2. The methylated oligosaccharides were converted to their corresponding partially methylated alditol acetates, and the products were analyzed by GC and GC–EIMS.[24]

2.5. Preparation of the alcohol insoluble residue of *Arabidopsis thaliana* rosette leaves

A. thaliana plants (ecotype columbia) were grown in potting soil in a growth chamber at 19 °C with 14 h of light and 15 °C with 10 h of dark. The rosette leaves were harvested from four-week-old plants. Rosette leaves were suspended in aqueous 80% ethanol and homogenized using a polytron disrupter. The suspension was filtered through nylon mesh, and the residue washed with aqueous 80% EtOH and then with EtOH. The residue was suspended in MeOH:chloroform (1:1 v/v, 500 mL) and stirred for 30 min at rt. The suspension was filtered through Whatmans No.1 paper, and the residue was washed with acetone. The residue, referred to as the 'alcohol-insoluble residue' (AIR), was then vacuum dried at rt.

2.6. Solubilization of pectic polysaccharides from *A. thaliana* AIR

The AIR (5 g) from *A. thaliana* plants was suspended in 50 mM NaOAc, pH 5 (250 mL), and hydrated for 4 h at rt. The suspension was treated for 16 h at 23 °C with homogeneous preparations of *Aspergillus aculeatus* pectin methylesterase (PME, 20 units; 1 unit releases 1 μmol MeOH/min), *A. niger* endopolygalacturonase (EPG, 15 units; 1 unit release 1 μmol reducing sugar/min), and *A. niger* exopolygalacturonase (ExoPG, 1 unit; 1 unit release 1 μmol reducing sugar/min). The suspension was filtered through nylon mesh, and the soluble material was concentrated to ~50 mL by rotary evaporation under reduced pressure, dialyzed (3500 MW cutoff) against deionized water, and freeze dried. The insoluble fraction was suspended in 50 mM NaOAc, pH 5, (200 mL) and treated with the same mixture of enzymes. The soluble material was then isolated and freeze-dried.

2.7. Isolation of RG-II from the EPG-soluble material

A solution of the combined EPG-soluble material (~ 350 mg) in 50 mM NaOAc, pH 5 (6 mL), was fractioned on a Sephadex G-75 column (3.3 × 100 cm) at 1.0 mL/min by elution with 50 mM NaOAc, pH 5.2. Fractions (3.5 mL) were collected, and portions (100 μL) were analyzed colorimetrically for uronic acid.[26] The RG-II-containing fractions were combined, dialyzed and freeze dried. The RG-II eluted predominantly as a single peak when analyzed by size-exclusion chromatography (SEC) on a Superdex-75 HR10/30 column eluted with 50 mM ammonium formate, pH 5.[9]

2.8. Generation of side chain B-enriched material from wine and *Arabidopsis* RG-II

Solutions of *A. thaliana* and red wine RG-II (~ 10 mg) in 0.1 M trifluroacetic acid (2 mL) were kept for 24 h at 40 °C.[4] The solutions were concentrated to dryness under a flow of air. MeOH (~ 1 mL) was then added, and the solution was concentrated to dryness. The residues were then dissolved in water and freeze-dried. Separate solutions of each residue in 50 mM ammonium formate, pH 5 (400 μL) were then fractionated by SEC using a Superdex-75 HR10/30 column.[9] The eluant was monitored with a Hewlett–Packard 5770A refractive index detector. Fractions were collected manually and repeatedly freeze-dried to remove the volatile ammonium salt.

2.9. Mass spectrometry

Electrospray-ionization mass spectrometry (ESIMS) was performed with a PE Sciex API III biomolecular analyzer operated in the positive-ion mode.[22] Solutions of oligosaccharides (100 μg) in 25% aq MeOH containing 0.5% HCl (100 μL) were infused into the electrospray source at 5 μL/min using a Harvard 22 syringe pump. The ion spray was operated at 5000 V with an orifice potential of 35 V. At least twenty scans (500–1500 amu) were collected and averaged. Matrix-assisted laser-desorption time-of-flight mass spectrometry (MALDI-TOF-MS) was performed with a HP G2025A LD-TOF system in the positive-ion mode and with 0.5% dihydroxybenzoic acid as the matrix.

2.10. NMR spectroscopy

Fraction 4 (6 mg) was dissolved in 99% D_2O (5 mL) and freeze-dried. The residue was dissolved in 99.9% D_2O (0.5 mL) and Na_2CO_3 (1 mg) was added. The pH of the solution was initially adjusted to 6.5 by bubbling with CO_2. Data were collected on Varian Inova 600 and 800 MHz spectrometers at 11, 25 and 60 °C. Gradient versions of COSY, HSQC,[27] HSQC–TOCSY[28] and TOCSY,[29,30] HMBC,[31] and NOESY[32] experiments were performed using standard Varian pulse sequences. Data from non-gradient HSQC and selective one-dimensional TOCSY[33,34] experiments were also collected. Data were processed with Varian and Felix (Molecular Simulations, Inc.) software.

The COSY spectra were collected with 400 × 2048 complex points and a spectral width of 8 ppm. The data were processed with shifted squared sinebell window functions, and zero filled to obtain a 2048 × 2048 matrix. The TOCSY and NOESY spectra were 256 × 2048 complex points, with mixing times of 100 and 200 ms, respectively. Heteronuclear spectra were recorded with 128 or 256 × 1024 complex points covering 120 ppm in the ^{13}C dimension. These data were processed typically with gaussian window functions and zero filling to obtain a 1024 × 2048 matrix. The chemical shifts were measured relative to internal acetone with ^1H at δ 2.22 and ^{13}C at δ 33.0.[35]

3. Results

The results described below confirm that the major oligosaccharide isolated as 'Fraction 4' is a heptasaccharide with structure **1**.

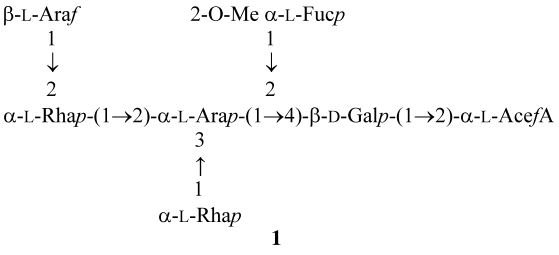

1

3.1. Glycosyl residue and linkage compositions of the oligoglycose present in Fraction 4

Partial acid hydrolysis of red wine RG-II followed by SEC and semipreparative HPAEC gave a product (Fraction 4) that contained Rha, Ara, Gal, 2-*O*-MeFuc and AceA in the molar ratios 2.3: 2.1: 0.9: 1.0: 0.4. The AceA content of Fraction 4 is underestimated due to its low recovery using the alditol acetate procedure.[16] Fraction 4 was shown, by glycosyl-linkage composition analysis, to contain equimolar amounts of nonreducing terminal Ara*f*, 2-*O*-MeFuc*p* and Rha*p*, 2-linked Rha*p*, 2,3-linked Ara*p*, and 2,4-linked Gal*p*. Somewhat lower amounts of 2-linked Ace*f*A were also detected. The ESI mass spectrum of Fraction 4 contained ions at m/z 1057 and 1079, corresponding to the $[M + H]^+$ and $[M + Na]^+$ ions, respectively, of a heptasaccharide composed of two rhamnosyl, two arabinosyl, one galactosyl, one 2-*O*-methylfucosyl, and one reducing aceric acid residue.

Aceric acid was the only deuterium-labeled alditol detected by glycosyl-residue composition analysis of $NaBD_4$-reduced Fraction 4 thereby establishing that AceA is present at the reducing end of the oligoglycose in this fraction. This result is in contrast to previous studies showing that oligoglycoses terminated at their reducing end with apiose are generated by treating RG-II for 24 h at 40 °C with 0.1 M TFA.[4,22] We assume that the oligoglycose in Fraction 4 was generated by hydrolysis of the glycosidic linkage between the 2-linked Ace*f*A residue and the 3-linked Rha*p* residue when RG-II was treated with aq 2% HOAc for 1.5 h at 100 °C. Nevertheless, these results, when taken together with the results of glycosyl-linkage composition analysis and the results of previous studies,[1,6,22] suggest that the major oligosaccharide in Fraction 4 is structure **1**.

3.2. ^{1}H and ^{13}C NMR spectroscopic characterization of 1

The complete ^{1}H and ^{13}C chemical shift values for the heptasaccharide **1** at 60 °C are given in Tables 1 and 2. Fig. 1 shows the anomeric and ring regions of an ^{1}H{^{13}C}–HSQC spectrum at 60 °C, and all signals from the seven glycosyl residues are labeled. Spectra were assigned from conventional two-dimensional homo- and heterocorrelated spectra, and in general chemical shifts matched literature values.[1,36] The 2-linked α-aceric furanuronosyl residue has no proton on C-3, and so the two proton pairs of H-1–H-2 and H-4–H-5 were connected via the HMBC spectrum (data not shown). There was no evidence of two anomeric forms of the aceric acid despite its being at the reducing end. The chemical shift (δ 5.65) of the anomeric proton of the α-2-*O*-methylfucopyranosyl residue (F1 in Fig. 1) was unusually downfield, but its connectivity in TOCSY and HMBC spectra, and the chemical shifts for the remainder of the spin system were consistent with the assignment. The terminal arabinosyl residue was confirmed to be a furanose from its C-4 chemical shift value of δ 84.1.

The glycosidic linkages in **1** were all confirmed by HMBC and NOESY data, as well as by characteristic carbon chemical shifts of linked carbons. In the HMBC spectrum, direct *trans*-glycosidic connectivity was seen between H-1 of the galactopyranosyl residue and C-2 of the aceric acid, between H-1 of the fucopyranosyl and C-2 of the galactopyranosyl residues, and between H-1 of the terminal arabinofuranosyl and C-2 of the 2-linked rhamnosyl residues. NOESY crosspeaks were seen between these linkages, as well as between H-1 of the 2-linked rhamnosyl and C-2 of the 2,3-linked

Table 1
^{1}H NMR chemical shifts and $^3J_{HH}$ values for heptasaccharide **1**

Residue	H-1	H-2	H-3	H-4	H-5	H-6
-2)-L-Ace*f*A	5.22 [a] (4.7)[b]	4.45	NA	4.39	1.14	
-2,4)-β-D-Gal*p*	4.66 (7.8)	3.67	3.96	3.96	3.70	3.86, 3.77
α-L-2-O-Me-Fuc*p*	5.65 (3.7)	3.45	4.00	3.81	4.37	1.17 (3.47 –OMe)
-2,3)-α-L-Ara*p*	5.04 (3)	4.05 (4)	3.96 (5)	4.06 (8,4)	3.90, 3.58 (10)	
α-L-Rha*p*	5.01 (1.5)	4.12	3.82	3.47	3.85	1.27
-2)-α-L-Rha*p*	5.07 (1.3)	3.98	3.77	3.43	3.76	1.28
β-L-Ara*f*	5.09 (4.7)	4.13	4.18	3.89	3.79, 3.69	

[a] D_2O at 60 °C, in ppm relative to DSS, measured from internal acetone at 2.22 ppm.
[b] $^3J_{HH}$ values in Hz, measured at 25 °C; values for 2,3-linked Ara*p* measured at 60 °C.

Table 2
^{13}C NMR chemical shifts and $^1J_{CH}$ values for heptasaccharide **1**

Residue	C-1	C-2	C-3	C-4	C-5	C-6
-2)-L-Ace*f*A	96.6 [a] (181) [b]	85.3	84.7	82.5	18.6	
-2,4)-β-D-Gal*p*	103.7 (164)	75.6	77.4	78.3	77.2	63.9
α-L-2-O-MeFuc*p*	97.6 (176)	79.9	70.7	74.4	68.8	17.9 (59.8 –OMe)
-2,3)-α-L-Ara*p*	102.7 (173)	74.8	75.9	67.4	63.6	
α-L-Rha*p*	101.2 (172)	72.5	72.8	74.6	71.3	19.2
-2)-α-L-Rha*p*	100.5 (173)	80.2	71.9	74.8	72.2	19.2
β-L-Ara*f*	103.6 (179)	78.8	75.2	84.1	63.4	

[a] D_2O at 60 °C, in ppm relative to DSS, measured from internal acetone at 33.0 ppm.
[b] $^1J_{CH}$ values in Hz measured at 25 °C; values for 2,3-linked Ara*p* measured at 60 °C.

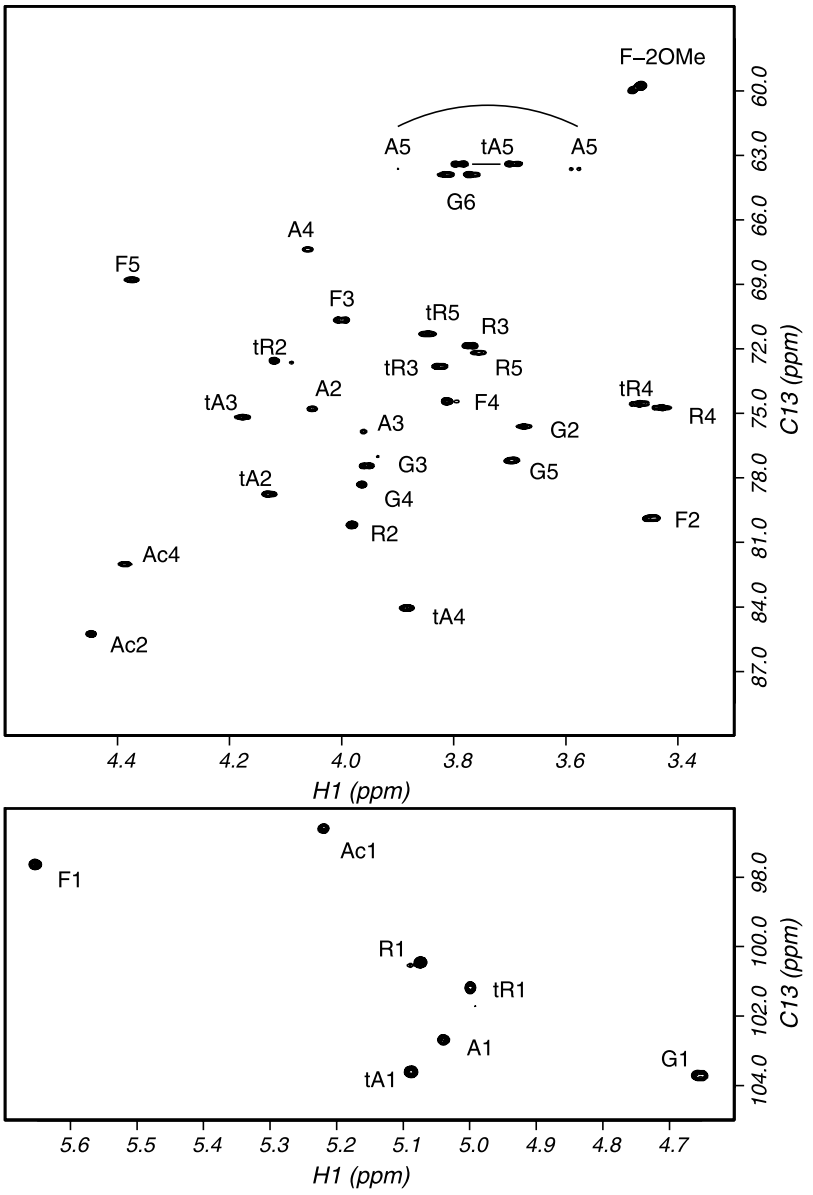

Fig. 1. Regions of the 600-MHz $^{1}H\{^{13}C\}$ HSQC spectrum of heptasaccharide **1** at 60 °C. Top panel, ring carbons; bottom panel, anomeric carbons. (Ac)Ace*f*A; (G)Gal*p*; (F)2-OMeFuc*p*; (A)Ara*p*; (R)Rha*p*; (tR) terminal-Rha*p*; (tA) terminal-Ara*f*.

arabinopyranosyl residues, and H-1 of the terminal rhamnosyl and C-3 of the 2,3-linked arabinospyranosyl residues. A NOESY crosspeak was observed between H-1 of the 2,3-linked arabinopyranosyl and the overlapping H-3 and H-4 of the galactopyranosyl residue; however, the chemical shifts for H-4 and C-4 of the galactopyranosyl residue (Tables 1 and 2) confirm the 4-linkage.[37]

Anomeric configurations were determined by $^{3}J_{HH}$ and $^{1}J_{HC}$ scalar coupling constants (Tables 1 and 2), as well as characteristic chemical shifts.[1,36] Fig. 1 shows low-intensity crosspeaks for the 2,3-linked arabinopyranosyl residue (e.g., A3 and A5), and their linewidths and chemical shifts change with temperature, suggesting some conformational averaging (Fig. 2). This is not unexpected since arabinopyranose can exist in both $^{1}C_{4}$ and $^{4}C_{1}$ chair conformers (Fig. 3).[38] The $^{1}C_{4}$ α-L-configuration best fits the measured scalar coupling constants (Tables 1 and 2), but there was also the possibility of a β-L-arabinopyranose structure (Fig. 3) averaging between a distorted $^{4}C_{1}$ and perhaps other non-chair conformations. Therefore, the α-L configuration was independently confirmed by examining a second oligosaccharide fragment.

3.3. Evidence that side chain B of wine RG-II contains a 2,3-linked α-L-Ara*p* residue

Side chain B contains four glycosyl residues (3-linked β-L-Rhap, 2-linked α-L Ace*f*A, 2,4-linked β-D-Gal*p*,

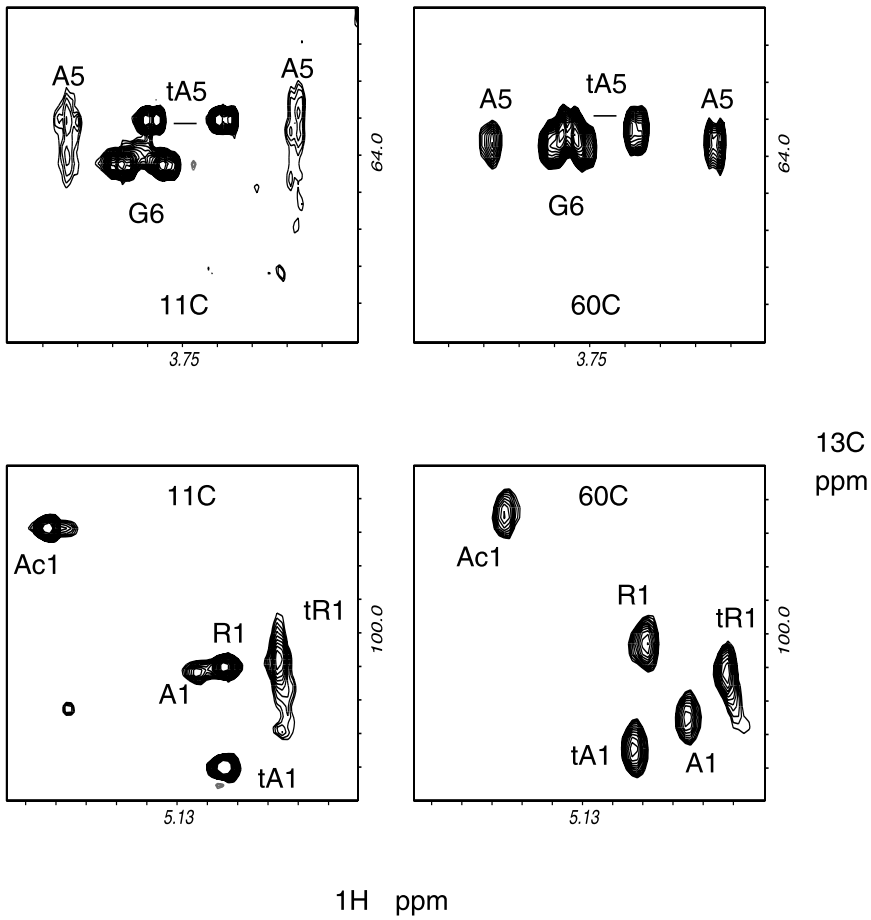

Fig. 2. Regions of 800-MHz $^{1}H\{^{13}C\}$ HSQC spectra of heptasaccharide **1** at 11 and 60 °C. The top panels show the broadening of the C-5 resonance (peaks A5) of arabinopyranose at lower temperatures. The bottom panels show a large temperature-dependent chemical shift of the arabinopyranosyl H-1 and C-1 (peak A1).

and 2,3-linked L-Ara*p*) that are resistant to periodate oxidation and five glycosyl residues (3′-linked β-D-Api*f*, T 2-*O*-Me α-L-Fuc*p*, T β-L-Ara*f*, T α-L-Rha*p* and 2-linked α-L-Rha*p*) that are susceptible to periodate oxidation (Fig. 4). Thus, we anticipated that Smith degradation of RG-II would generate a tetraglycosyl alditol containing the periodate-resistant Ara*p*, β-Gal*p*, β-Ace*f*, and β-Rha*p* residues together with a three-carbon fragment (glycerol) that is formed by periodate oxidation of a 3′-linked β-D-Api*f* residue (see Fig. 4). The unsubstituted Ara*p* residue is at the nonreducing terminus of the tetraglycosyl alditol and most likely adopts the $^{4}C_{1}$ chair conformation that is characteristic of free arabinopyranose.

Smith degradation of RG-II followed by anion-exchange chromatography of the products on Q-Sepharose gave a fraction that was rich in Ara, Gal, Rha, AceA, and glycerol. This fraction was then separated into two major components (S1 and S2) by semipreparative HPAEC–PAD (data not shown). Fraction S1 contained a mixture of oligosaccharides and was not further analyzed. The MALDI-TOF mass spectrum of

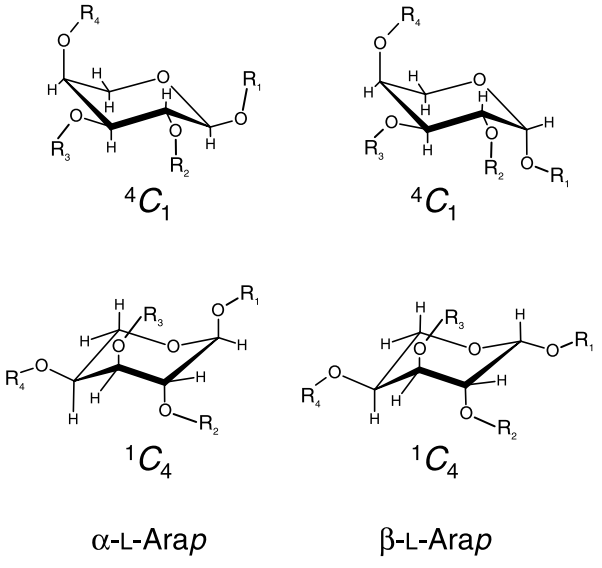

Fig. 3. Chair forms of α-L- and β-L-arabinopyranose.

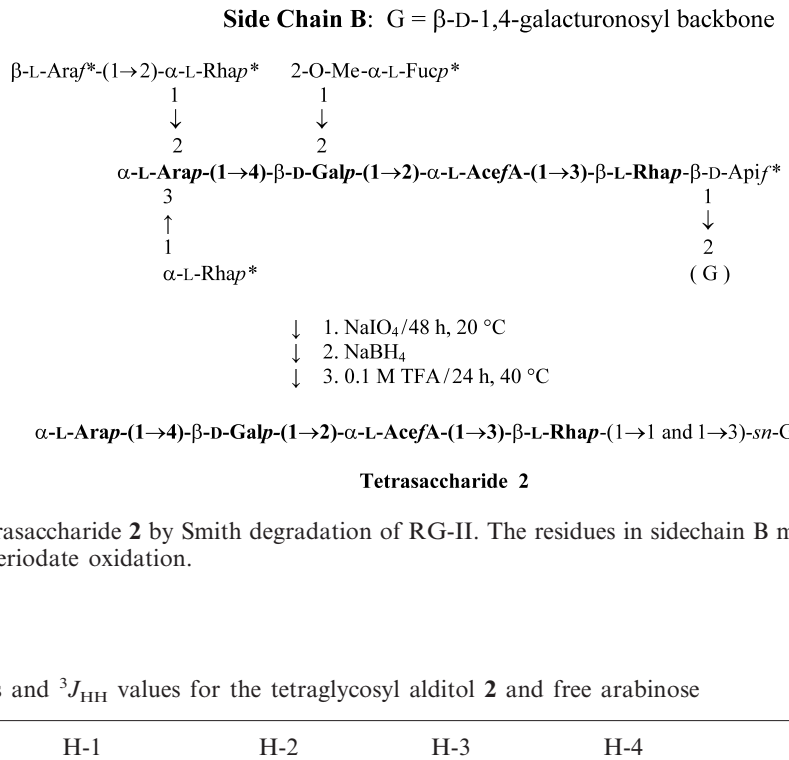

Fig. 4. Generation of tetrasaccharide **2** by Smith degradation of RG-II. The residues in sidechain B marked with an asterisk have cis-diols susceptible to periodate oxidation.

Table 3
^{1}H NMR chemical shifts and $^{3}J_{HH}$ values for the tetraglycosyl alditol **2** and free arabinose

Residue	H-1	H-2	H-3	H-4	H-5	H-6
α-L-Ara*p*	4.54 [a] (7.7)[b]	3.58 (9.8)	3.65 (3)	3.90 (<2)	3.89, 3.61	–
-4)-β-D-Gal*p*	4.52 (7.8)	3.66 (9.8)	3.73 (3.2)	4.12 (<2)	3.71	3.80
-2)-α-L-Ace*f*	5.38 (5.0)	4.39	–	4.84 (6.5)	1.19	–
-3)-β-L-Rha*p* (form 1)	4.86 (<2)	4.18 (3)	3.89 (10)	3.57 (10)	3.75 (6.3)	1.31
-3)-β-L-Rha*p* (form 2)	4.87 (<2)	4.19 (3)	3.89 (10)	3.57 (10)	3.75 (6.3)	1.31
-3)-Gro (form 1)	3.57 [c] (4)	3.91	3.66	–	–	–
	3.72 [c] (6)		3.57			
-3)-Gro (form 2)	3.48 [c] (6)	3.91	3.66	–	–	–
	3.78 [c] (4)		3.57			
Free α-L-Ara*p*	4.49 (7.8)	3.49 (9.9)	3.64 (3.6)	3.92 (2.1, <2)	3.88, 3.66	–
Free β-L-Ara*p*	5.22 (3.6)	3.80 (9.8)	3.86 (3.4)	3.98 (1.5, 2.5)	4.01, 3.63	–

[a] D_2O at 25 °C, in ppm from DSS, measured from internal acetone at 2.22.
[b] $^{3}J_{HH}$ values in Hz.
[c] The absolute stereochemistry of the two different glycerol aglycons was not determined, so the carbon bearing the glycosidic substituent is arbitrarily designated as C-1. Further analysis of stereochemistry would allow these carbons to unambiguously assigned as *sn*-3 or *sn*-1.

Table 4
^{13}C NMR chemical shifts for the tetraglycosyl alditol **2** [a]

Residue	C-1	C-2	C-3	C-4	C-5	C-6
α-L-Ara*p*	105.0	72.1	73.0	69.0	67.1	–
-4)-β-D-Gal*p*	104.5	71.5	73.7	77.2	75.4	61.3
-2)-α-L-Ace*f*	98.4	88.4		78.5	13.3	–
-3)-β-L-Rha*p* (form 1)	100.5	67.4	76.8	70.7	69.2	17.5
-3)-β-L-Rha*p* (form 2)	100.0	67.4	76.8	70.7	69.2	17.5
-3)-Gro (form 1)	68.8	71.0	63.0	–	–	–
-3)-Gro (form 2)	69.1	71.0	63.0	–	–	–

[a] D_2O at 25 °C, in ppm from DSS, measured from internal acetone at 33.0 ppm.

S2 contained ions at m/z 693 and 715 corresponding to $[M+H]^+$ and $[M+Na]^+$, respectively, of a tetraglycosyl alditol (**2**) composed of one Ara, one Gal, one Rha, and one aceric acid residue, and glycerol:

α-L-Ara*p*-(1→4)-β-D-Gal*p*-(1→2)-α-L-Ace*f*A-(1→3)-β-L-Rha*p*-(1→3)-Gro*a*
2

The resonances in the ^1H (Table 3) and ^{13}C (Table 4) NMR spectra of **2** were assigned by standard 2-dimensional NMR spectroscopic techniques. Two sets of resonances for glycerol and two sets of resonances for the β-Rha*p* residue, which is directly linked to glycerol, are present in the ^1H and ^{13}C spectra of **2** (see Tables 3 and 4). This result was expected because **2** is a mixture of two diastereomeric compounds that differ in the absolute configuration of the aglycon (1-*sn*-glycerol vs. 3-*sn*-glycerol). These two diastereoisomers are formed by the nonstereospecific reduction of the ketone (dihydroxyacetone) generated by periodate oxidation of C-3 of the β-Api*f* residue.

The ^1H spectrum of **2** contained resonances at δ 4.52 and δ 4.54 that were assigned to the anomeric protons of β-Gal*p* and α-Ara*p* residues, respectively. A long-range interglycosidic scalar coupling between H-1 of the α-Ara*p* residue and H-4 of the β-Gal*p* residue was clearly visible in the high-resolution gCOSY spectrum[39] and confirmed that the anomeric resonance at δ 4.52 originated from the α-Ara*p* residue. The resonances of H-2 through H-4 of the β-Gal*p* and α-Ara*p* spin systems were readily traced in the COSY and TOSCY spectra of **2**. The scalar coupling network of the α-Ara*p* and β-Gal*p* residues of **2** could not be unambiguously traced beyond H-4 because of signal overlap and the small magnitude of $^3J_{H4,H5}$ for these spin systems. Therefore, the H-5_{ax} and H-5_{eq} resonances of the terminal α-Ara*p* residue were assigned by reference to the ^1H spectra of arabinose (see Table 3). This also allowed the resonances corresponding to H-5, H-6 and H-6′ of the β-Gal*p* residue to be assigned by process of elimination.

The anomeric configuration and ring conformation of an arabinopyranosyl residue is readily determined by measuring its $^3J_{H,H}$ scalar coupling constants. As Table 3 indicates, $^3J_{H1,H2}$ and $^3J_{H2,H3}$ are both greater than 7 Hz, characteristic of the *trans*-diaxial arrangement of H-1, H-2 and H-3 in a $^4C_1$ chair conformation, and thus confirms the α-Arap configuration (Fig. 3).

3.4. Side chain B of wine RG-II is a nonasaccharide

The primary structures of heptasaccharide **1** and the tetraglycosyl alditol **2**, together with the primary structure of a enzymically-generated undecaglycosyl alditol[1] provide compelling evidence that in wine RG-II side chain B is the nonasaccharide **3**:

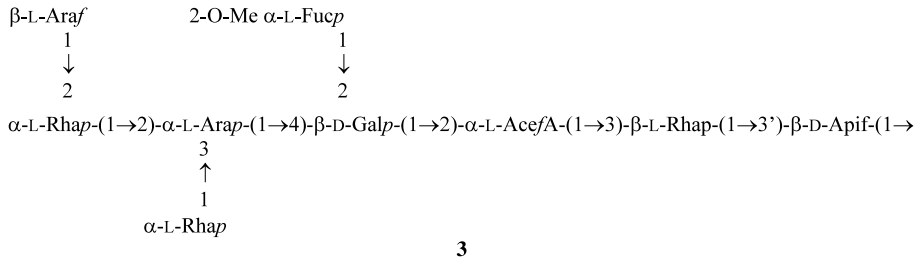

3

3.5. The number of glycosyl residues differ in the aceric acid-containing side chain generated from *Arabidopsis* leaf RG-II and wine RG-II

We have provided evidence that in wine RG-II side chain B is a nonasaccharide (**3**). However, the results of other studies[40–44] have suggested that the number of glycosyl residues in this side chain may vary depending on plant source. Thus, we compared the structures of side chain B that were released by treating *A. thaliana* rosette leaf and red wine RG-II for 24 h at 40 °C with 0.1 M TFA. This treatment has been shown to selectively hydrolyze the apiosidic linkage of side chain B.[4] *A. thaliana* RG-II was chosen, as this plant has become a model system in numerous areas of plant biology research.[45]

The side chain B-enriched material obtained from wine RG-II (W1) contained Api, Rha, Ara, Gal, MeFuc, and AceA in the molar ratios of 1.0: 2.8: 2.1: 1.3: 1.0:0.8, whereas the corresponding material from Arabidopsis (AT1) contained Api, Rha, Ara, Gal, MeFuc, and AceA in the molar ratios of 1.0:1.7: 1.5: 1.5: 0.9:0.8. Such a result indicated that the number of rhamnosyl and arabinosyl residues differ in side chain B from Arabidopsis and wine RG-II. To confirm and extend this observation we used ESIMS to determine the number of glycosyl residues in these side chains and the extent to which these side chains are *O*-acetylated.

The ESI mass spectrum of Fraction AT1 (Fig. 5A) contained ions at m/z 953 and 995 corresponding to $[M+H]^+$ from a mono- and di-*O*-acetylated hexasaccharide composed of one Api, one Rha, one AceA, one Gal, one Ara, and one 2-*O*-MeFuc residue. The ESI mass spectrum also contained ions at m/z 1099 and 1141 corresponding to $[M+H]^+$ from a mono- and di-*O*-acetylated heptasaccharide composed of one Api,

two Rha, one AceA, one Gal, one 2-*O*-MeFuc, and one Ara residue. Protonated molecular ions corresponding to the hexa- and heptasaccharide and their mono- and di-*O*-acetylated derivatives were also present in the ESI mass spectrum of Fraction W1 (Fig. 5B). This spectrum also contained ions at *m*/*z* 1203, 1245, and 1287 corresponding to $[M+H]^+$ from a octasaccharide and its-mono- and di-*O*-acetylated derivatives, respectively. These octasaccharides are likely to contain one additional Rha residue because their masses are 146 amu greater than the corresponding heptasaccharides. The ion at *m*/*z* 1231 also corresponds to $[M+H]^+$ from a mono-*O*-acetylated octasaccharide. However, this mass is 132 amu greater than the mono-*O*-acetylated heptasaccharide. An increase in mass of 132 amu corresponds to the addition of one Ara residue. The ions at *m*/*z* 1335, 1377, and 1419 correspond to $[M+H]^+$ of a nonasaccharide and its mono- and di-*O*-acetylated derivatives, respectively. These nonasaccharides are most likely formed by the addition one Rha (146 amu) and one Ara (132 amu) residue to the heptasaccharide.

We have shown that partial acid hydrolysis of wine RG-II generates aceric acid-containing hexa-, hepta-, octa, and nonasaccharides and their mono and di-*O*-acetylated derivatives. Oligosaccharides with a DP between 6 and 8 could be generated by partial acid hydrolysis of the nonasaccharide. Nevertheless, the possibility cannot be discounted that the 6-, 7-, 8-, and 9-mer are genuine side chains of wine RG-II. In contrast, no discernible amounts of octa and nonasaccharide were generated by partial acid hydrolysis of RG-II isolated from Arabidopsis rosette leaf cell walls. Moreover, no octa- or nonasaccharides were generated by 0.1M TFA treatment of RG-II isolated from the Arabidopsis *mur1–2* mutant, and RG-II isolated from the walls of suspension-cultured Arabidopsis cells (M.A. O'Neill, unpublished results). It is unlikely that the octa- and nonasaccharides were hydrolyzed to the heptasaccharide by contaminating glycanses in the EPG and PME used to release RG-II from Arabidopsis walls because treating wine RG-II with these enzymes had no discernible effect on the structure of side chain B (data not shown). Thus, we conclude that it is unlikely that quantitatively major amounts of aceric acid-containing octa- and nonasaccharide are present in Arabidopis RG-II.

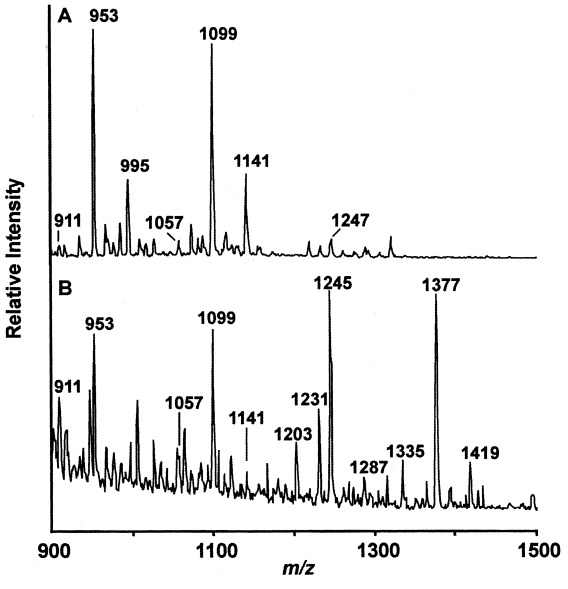

Fig. 5. ESI mass spectra of the side chain B-enriched fraction generated from Arabidopsis and wine RG-II. (A) Arabidopsis RG-II; (B) wine RG-II.

4. Discussion

The primary sequence of the aceric acid-containing nonasaccharide **3** that is linked to the backbone of red wine RG-II has been determined. Our data establish that the α-L-Ara*p* residue is substituted at C-3 with a nonreducing terminal α-L-Rha*p* residue and at C-2 with the disaccharide β-L-Ara*f*-(1→2)-α-L-Rha*p*. Our data also confirm a previous report[1] that showed that side chain B contains a 2,4-linked β-D-Gal*p* residue and a 2-linked α-L-Ace*f*A residue. The ^{13}C and ^{1}H NMR resonances have been completely assigned for the heptasaccharide derived from side chain B by hydrolysis at aceric acid. This extends and corrects assignments for side chain B resonances given in a previous report on intact RG-II.[12]

The primary structure determination of side chain B is the first step toward a detailed conformational analysis of RG-II. An unambiguous primary structure for the 2-O-Me-xylose-containing side chain remains to be determined, as does the precise location of each of the four side chains along the homogalacturonan backbone.

4.1. The α-L-Ara*p* ring is conformationally flexible

The NMR data suggests that the 2,3-linked arabinopyranosyl residue is flexible, consistent with other studies that have reported dynamic conformational processes for arabinopyranosyl residues. For example, the $^{1}C_4$ conformer is believed to be the predominant form of the 2-linked α-L-arabinopyranosyl residue in saponins isolated from *Platycodon grandiflorum*.[38] The equilibrium is shifted toward the $^{4}C_1$ conformer by O-acetylation. Our NMR scalar coupling data for **1** ($^{1}J_{C1,H1} = 173$, $^{3}J_{H1,H2} = 3$, $^{3}J_{H3,H4} = 5$, and $^{3}J_{H4,H5} = 8$ Hz) are consistent with the presence of a branched Ara*p* residue that exists predominantly, but not solely in the $^{1}C_4$ chair conformation (see Fig. 3). In contrast, the terminal nonreducing Ara*p* residue in **2** exists predominantly in the $^{4}C_1$ chair conformation. The ^{13}C line

widths of the Ara*p* H-5$_C$/H-5′$_C$ cross peaks in the HSQC of **1** (Fig. 2) are broadened at temperatures below 60 °C, indicative of a chemical shift difference between the conformers that puts the exchange process at an intermediate rate on the NMR time scale. Interestingly, the proton linewidths are less affected. As the chemical shift of C-5 in a pyranose is known to be sensitive to the axial or equatorial position of the anomeric oxygen (the 'gauche-effect'),[37] this broadening may result from a movement of the anomeric center relative to C-5. Furthermore, the steric interactions between the glycosyl substituents at C-1, C-2 and C-3, on this highly substituted Ara*p* residue may prevent the ring from adopting a single stable conformation.

4.2. Variations in the length of side chain B

Side chain B has been reported to exist as a hepta-, octa-, and nonasaccharide in the walls of suspension-cultured sycamore (*Acer pseudoplatanus*) RG-II[22] and as a nonasaccharide in ginseng (*Panax ginseng*) leaf RG-II.[40] Our data show that this side chain is a nonasaccharide in red wine RG-II and a heptasaccharide in Arabidopsis RG-II. Side chain B has been reported to be an octasaccharide in bamboo (*Phyllostachys edulis*) shoot RG-II,[41] and as a hexasaccharide in the RG-II isolated from sugar beet (*Beta vulgaris*) pulp,[42] akamutsu (*Pinus densiflora*) hypocotyls,[43] and red beet (*Beta vulgaris* L var *conditiv*a) tubers.[44] Thus, the number of glycosyl residues in this side chain may vary depending on the plant source, although the possibility cannot be discounted that these structural variations result from differences in the procedures used to chemically fragment and isolate RG-II oligosaccharides. Nevertheless, the limited data available suggest that the structural variations result from the presence or absence of substituents linked to C-2 and/or C-3 of the Ara*p* residue. This residue is 2,3-linked in red wine[6] and ginseng RG-II,[40] but is 2-linked in Arabidopsis RG-II and has been reported to be present as a terminal nonreducing residue in sugar beet[42] and red beet RG-II.[44] Thus, some plants may lack the glycosyl transferases required to add the Ara*f* and Rha*p* residues to the Ara*p* residue. Alternatively, all plants may synthesize a nonasaccharide, but only some of them may produce exoglycanases that 'trim' the nonasaccharide to smaller oligosaccharides.

The complex primary structure of RG-II is conserved in higher plants. Moreover, in all plants that have been examined to data at least 95% of the RG-II in the primary wall is present as a dimer that is cross-linked by borate. This cross-link is required for normal plant growth because a reduction in the extent of cross-linking of RG-II in the Arabidopsis *mur1* mutant is in large part responsible for the dwarf phenotype of this plant.[12] Reduced RG-II crosslinking occurs as a result of replacing L-fucosyl residues (in wild-type plants) with L-galactosyl residues (in *mur1* plants). Thus, the glycosyl sequence and the three-dimensional conformation of RG-II are likely to be important in regulating the interaction of this pectic polysaccharide with borate. It is likely that RG-II cross-linking in the walls of growing cells requires the precise positioning of the apiosyl residues of two RG-II molecules, together with the lowering of energetic barriers to borate diester formation. Although the Ara*p* residue discussed above is remote from the proposed borate crosslinking site in the primary sequence, its position in the three-dimensional structure is not known. Thus, the conformational transitions of the RG-II side chains required for the diester formation may depend in part on the conformational equilibrium of the Ara*p*. Additional research is required to determine the importance of the conformational flexibility of RG-II side chains in the cross-linking process.

Acknowledgements

Financial support from NIH resource center grant, RR05351, National Institute of General Medical Sciences grant, GM33225, and U.S. Department of Energy grants, DE-FG05-93ER20115 and DE-FG09-93ER20097 is acknowledged.

References

1. Vidal, S.; Doco, T.; Williams, P.; Pellerin, P.; York, W. S.; O'Neill, M. A.; Darvill, A. G.; Albersheim, P. *Carbohydr. Res.* **2000**, *326*, 277–294.
2. Darvill, A. G.; McNeil, M.; Albersheim, P. *Plant Physiol.* **1978**, *62*, 418–422.
3. O'Neill, M. A.; Darvill, A. G.; Albersheim, P. The pectic polysaccharides of primary cell walls. In *Methods in Plant Biochemistry*; Dey, P. M., Ed.; Academic Press: London, 1990; Vol. 2, pp 415–441.
4. Spellman, M. W.; McNeil, M.; Darvill, A. G.; Albersheim, P. *Carbohydr. Res.* **1983**, *122*, 131–153.
5. Doco, T.; Brilloutet, J.-M. *Carbohydr. Res.* **1993**, *243*, 333–343.
6. Pellerin, P.; Doco, T.; Vidal, S.; Williams, P.; Brilloutet, J.-M.; O'Neill, M. A. *Carbohydr. Res.* **1996**, *290*, 183–197.
7. Kobayashi, M.; Matoh, T.; Azuma, J. *Plant Physiol.* **1996**, *110*, 1017–1020.
8. Ishii, T.; Matsunga, T. *Carbohydr. Res.* **1996**, *284*, 1–9.
9. O'Neill, M. A.; Warrenfeltz, D.; Kates, K.; Pellerin, P.; Doco, T.; Darvill, A. G.; Albersheim, P. *J. Biol. Chem.* **1996**, *271*, 22923–22930.
10. Matoh, T. *Plant Soil* **1997**, *193*, 59–70.
11. Ishii, T.; Matsunaga, T.; Pellerin, P.; O'Neill, M. A.; Darvill, A. G.; Albersheim, P. *J. Biol. Chem.* **1999**, *274*, 13098–13104.
12. O'Neill, M. A.; Eberhard, S.; Albersheim, P.; Darvill, A. G. *Science* **2001**, *294*, 846–849.

13. Perez, S.; Mazeau, K.; du Penhoat, C. *Plant Physiol. Biochem.* **2000**, *38*, 37–55.
14. du Penhoat, C.; Gey, C.; Pellerin, P.; Perez, S. *J. Biol. NMR* **1999**, *14*, 253–271.
15. York, W. S.; Impallomeni, G.; Hisamatsu, M.; Albersheim, P. *Carbohydr. Res.* **1994**, *267*, 79–104.
16. Spellman, M. W.; McNeil, M.; Darvill, A. G.; Albersheim, P.; Henrik, K. *Carbohydr. Res.* **1983**, *122*, 115–129.
17. York, W. S.; Darvill, A. G.; McNeil, M.; Albersheim, P. *Carbohydr. Res.* **1985**, *138*, 109–126.
18. Stevenson, T. T.; Darvill, A. G.; Albersheim, P. *Carbohydr. Res.* **1988**, *179*, 269–288.
19. Stevenson, T. T.; Darvill, A. G.; Albersheim, P. *Carbohydr. Res.* **1988**, *182*, 207–226.
20. Puvanesarajah, V.; Darvill, A. G.; Albersheim, P. *Carbohydr. Res.* **1991**, *218*, 211–222.
21. Melton, L. D.; McNeil, M.; Darvill, A. G.; Albersheim, P. *Carbohydr. Res.* **1986**, *146*, 279–305.
22. Whitcombe, A. J.; O'Neill, M. A.; Steffan, W.; Albersheim, P.; Darvill, A. G. *Carbohydr. Res.* **1995**, *271*, 15–29.
23. Goldstein, I. J.; Hay, C. W.; Lewis, B. A.; Smith, F. *Methods Carbohydr. Chem.* **1965**, *5*, 361–370.
24. York, W.; Darvill, A. G.; Stevenson, T. T.; Albersheim, P. *Methods Enzymol.* **1986**, *118*, 3–40.
25. Ciucanu, I.; Kerek, F. *Carbohydr. Res.* **1984**, *131*, 209–217.
26. Blumenkrantz, N.; Asboe-Hansen, G. *Anal. Biochem.* **1973**, *54*, 484–489.
27. Davis, A. L.; Keeler, J.; Laue, E. D.; Moskau, D. *J. Magn. Reson.* **1992**, *98*, 207–216.
28. Lerner, L.; Bax, A. *J. Magn. Reson.* **1986**, *69*, 375–380.
29. Braunschweiler, L.; Ernst, R. R. *J. Magn. Reson.* **1983**, *53*, 521–528.
30. Bax, A.; Davis, D. G. *J. Magn. Reson.* **1985**, *65*, 355–360.
31. Bax, A.; Summers, M. F. *J. Am. Chem. Soc.* **1986**, 108.
32. Macura, S.; Ernst, R. R. *Mol. Phys.* **1980**, *41*, 95–117.
33. Dalvit, C.; Boverman, G. *Magn. Reson. Chem.* **1995**, *33*, 156–159.
34. Stonehouse, J.; Adell, P.; Keeler, J.; Shaka, A. J. *J. Am. Chem. Soc.* **1994**, *116*, 6037–6038.
35. Wishart, D. S.; Bigam, C. G.; Yao, J.; Abildgaard, F.; Dyson, H. J.; Oldfield, E.; Markley, J. L.; Sykes, B. D. *J. Biomol. NMR* **1995**, *6*, 135–140.
36. Bock, K.; Thorgersen, H. *Ann. Rep. NMR Spectrosc.* **1982**, *13*, 1–57.
37. Bock, K.; Pedersen, C. *Adv. Carbohydr. Chem. Biochem.* **1983**, *41*, 27–66.
38. Ishii, H.; Kitagawa, I.; Matsushita, K.; Shirakawa, K.; Tori, K.; Yoshikawa, M.; Yoshimura, Y. *Tetrahedron Lett.* **1981**, *22*, 1529–1532.
39. Otter, A.; Bundle, D. R. *J. Magn. Reson. Ser. B.* **1995**, *109*, 194–201.
40. Shin, K.-S.; Kiyohara, H.; Matsumoto, T.; Yamada, H. *Carbohydr. Res.* **1998**, *307*, 97–106.
41. Kaneko, S.; Ishii, T.; Matsunaga, T. *Phytochemistry* **1997**, *44*, 243–248.
42. Ishii, T.; Kaneko, S. *Phytochemistry* **1998**, *49*, 1195–1202.
43. Shimokawa, T.; Ishii, T.; Matsunaga, T. *J. Wood Sci.* **1999**, 45.
44. Strasser, G. R.; Amado, R. *Carbohydr. Polymers* **2002**, *48*, 263–269.
45. Arabidopsis 2000.The Arabidopsis Genome Initiative. Nature **2000**, *408*, 796–815.